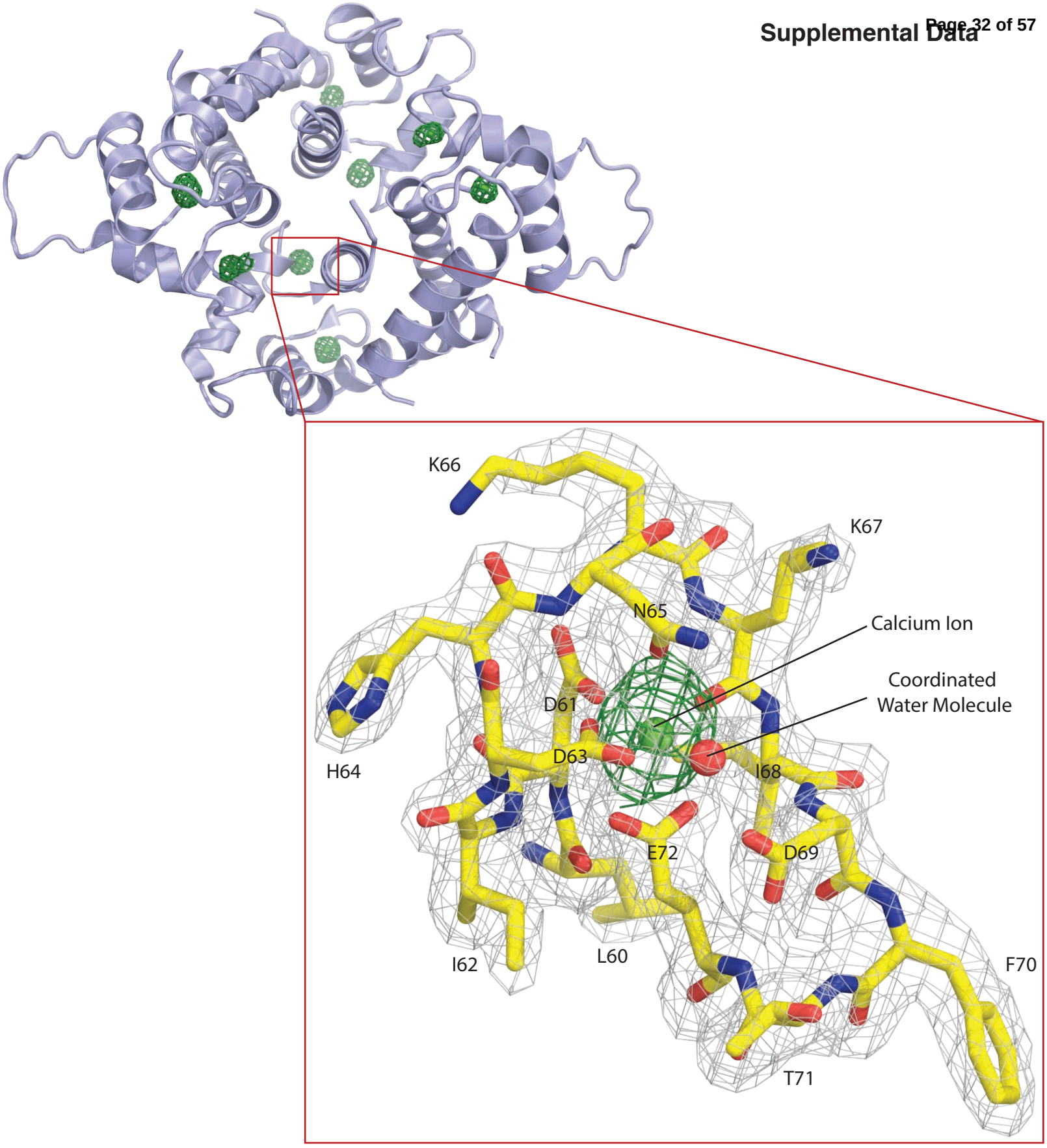

Figure S1 -- Unbiased Fo-Fc electron density of calcium ions. Profilaggrin crystal asymmetric unit (top; two dimers) in light blue with the eight bound calcium ions as green spheres. Depicted in green wire mesh is the Fo-Fc electron density contoured at 3σ. Pictured at the bottom right within the red zoom box is the canonical EF-hand in the C subunit, showing classic canonical EF-hand calcium coordination (residues labeled) and the Fo-Fc electron density in green (contoured at 3σ).

Canonical and Pseudo/S100 Calcium Binding Loops in Profilaggrin Crystal Structure

Profilaggrin Pseudo/S100 Calcium Binding Loop

Seq 18-	S	K	K	D	K	N	T	D	T	L	S	K	K	E -31
Position-	1	2	3	4	5	6	7	8	9	10	11	12	13	14

Positions 1, 6, 9: main chain oxygens coordinate Ca^{2+}
Position 4: monodentate Ca^{2+} coordination via side chain
Position 9: hydrogen-bonds to a HOH coordinating Ca^{2+}
Position 14: bidentate side chain coordination of Ca^{2+}

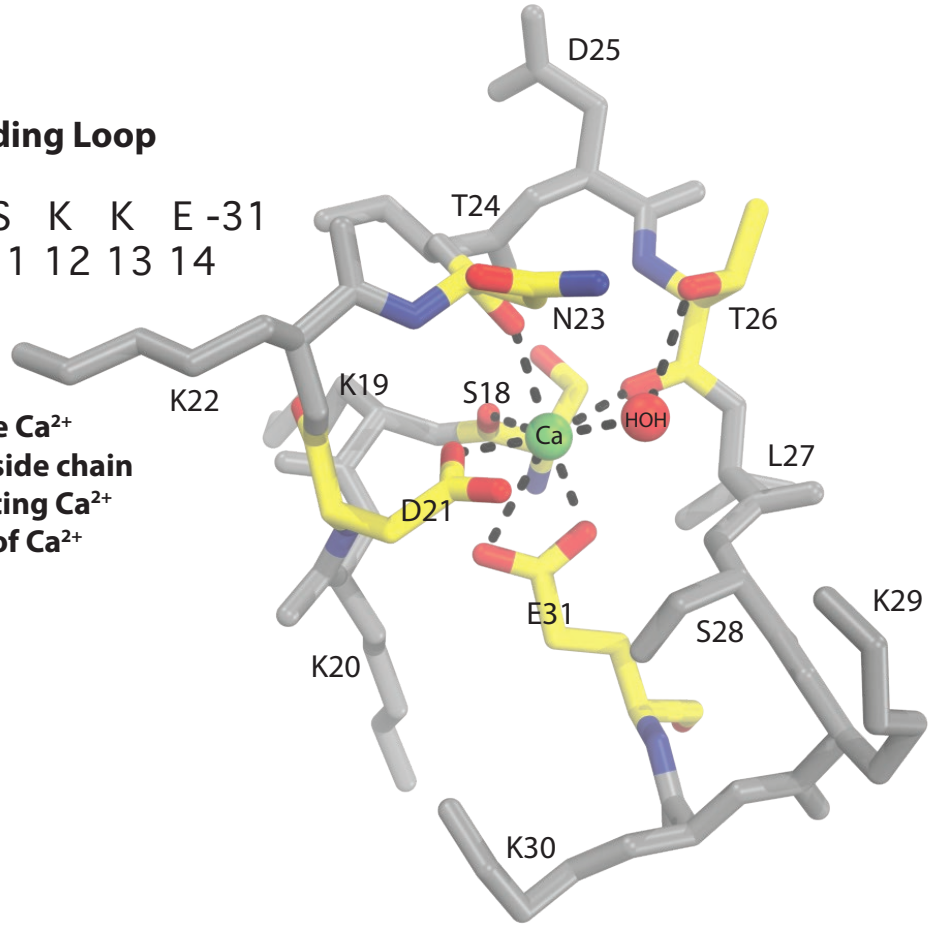

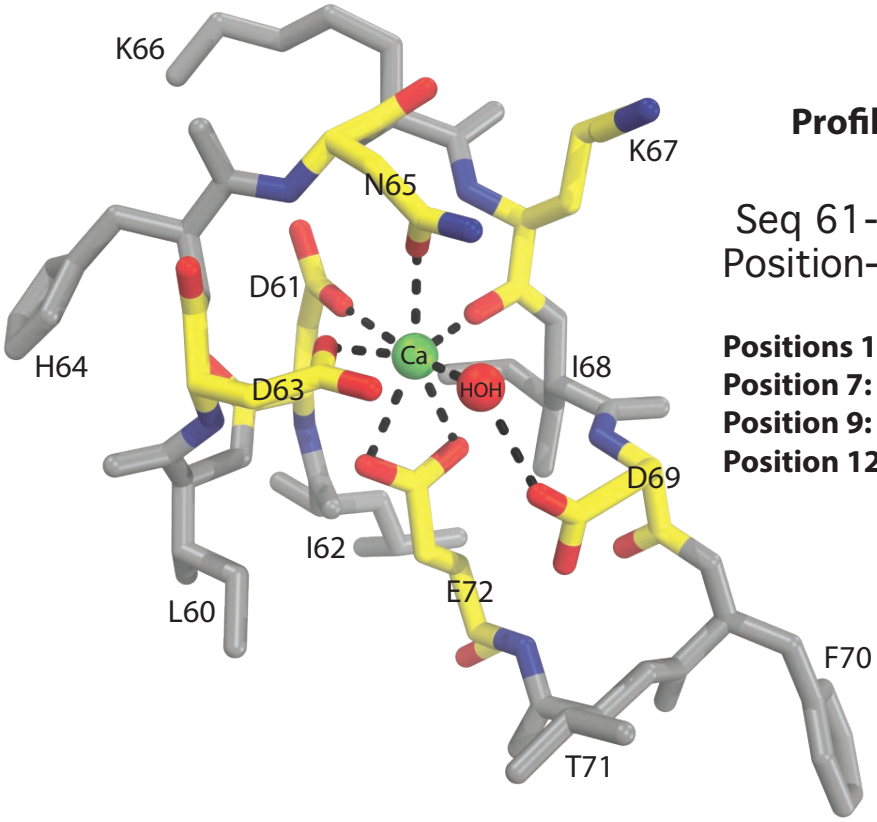

Profilaggrin Canonical Calcium Binding Loop

Seq 61-	D	I	D	H	N	K	K	I	D	F	T	E -72
Position-	1	2	3	4	5	6	7	8	9	10	11	12

Positions 1, 3, 5: monodentate Ca^{2+} coordination via side chains
Position 7: coordinates Ca^{2+} via main chain oxygen
Position 9: hydrogen-bonds to a HOH coordinating Ca^{2+}
Position 12: bidentate side chain coordination of Ca^{2+}

Figure S2 -- Calcium coordination. Profilaggrin, belonging to the S100 fused-type protein family, contains two types of EF-hands: an N-terminal pseudo/S100 (non-canonical) calcium binding loop (top) and a C-terminal canonical calcium binding loop (bottom). The profilaggrin sequence for each calcium binding loop in the N-terminal calcium binding domain is depicted, along with a position number. The type of calcium coordination for each position within the calcium binding loop is described for both types of calcium binding sites (pseudo/S100/non-canonical vs canonical). Images from the x-ray structure depict the pseudo/S100 (top) and canonical (bottom) calcium coordination for profilaggrin's N-terminus.

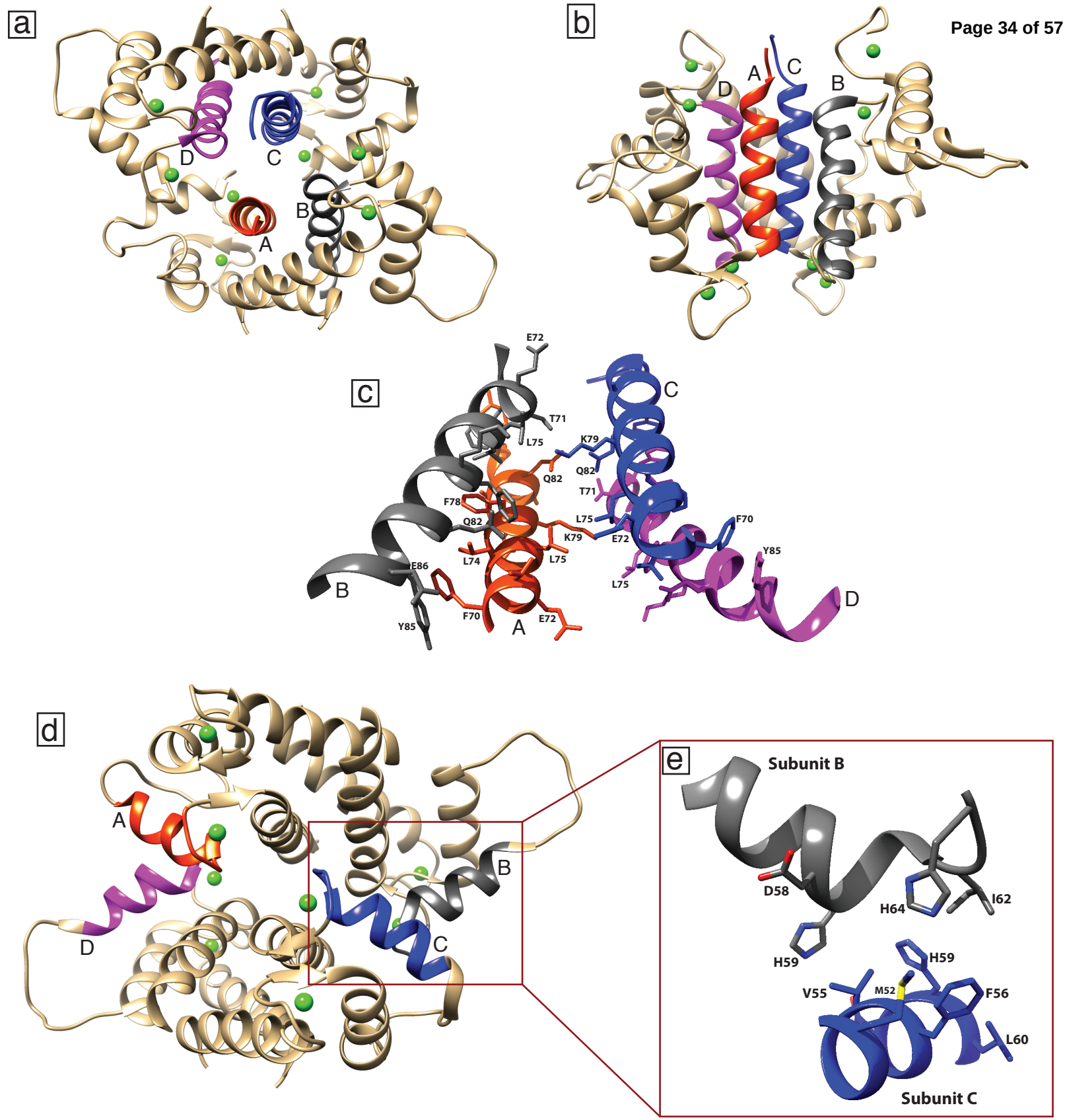

Figure S3 -- Inter-molecular interactions between helices IV (top) and helices III (bottom) stabilize the crystallized tetrameric aggregate. (a) Ribbon view of crystal AU, highlighting the helix IV interface between two PF-CABD dimers; helix IV for each subunit (A through D) is colored and labeled (A, red-orange; B, gray; C, blue; D, magenta). (b) Panel 'a' has been rotated 90° upward to show a side view of the tetrameric aggregate (helix I from the A and B subunits has been removed for clarity). (c) Focused view of the helix 4 interface, with residues most important for interface stablization shown as stick model. (d) Ribbon view of crystal AU, highlighting the helix III interface between two PF-CABD dimers; the same labeling and color scheme is used from the prior panels, but the colored helix is the 3rd helix, not helix IV as in panels a-c. (e) Focused view (rotated ~ 180° from panel d) of helix III interactions, with residues most important for interface stablization shown as stick model. The combined buried surface area is ~ 700 Å^2 for the helix IV interface and ~ 1000 Å^2 for the helix III interface. Calcium ions are depicted as green spheres.

Supplemental Data

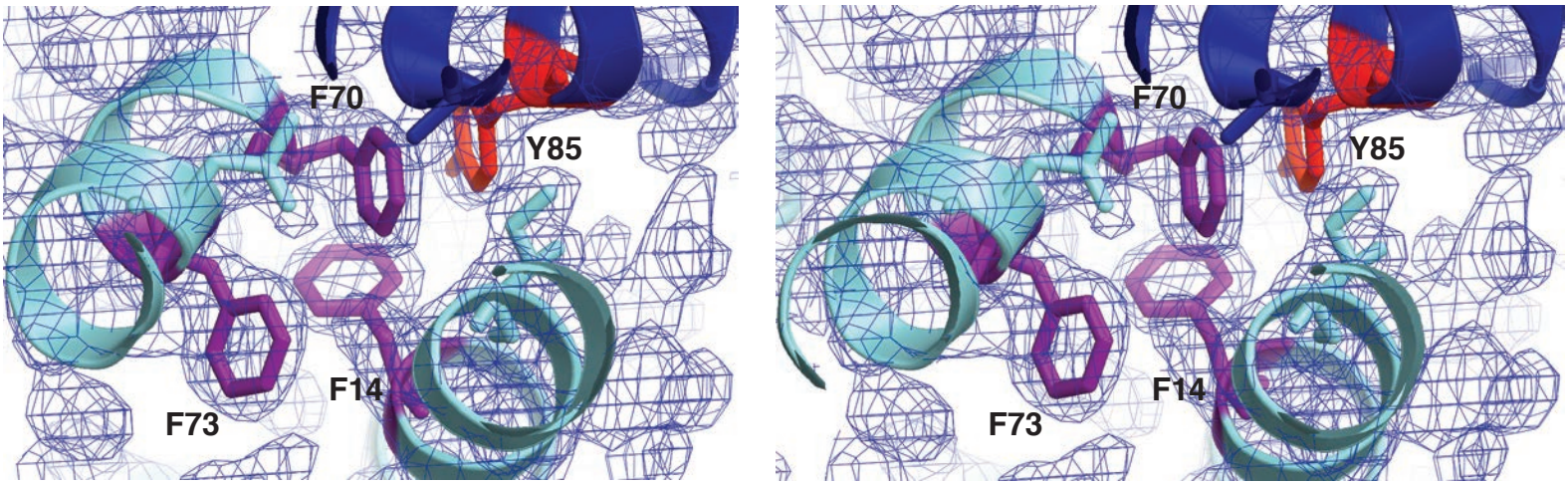

Figure S4, related to Figure 2. Stereo image of the electron density for the four aromatic ring cluster present in the N-terminus of profilaggrin. Tyr85 (red) of one monomer (dark blue) stacks against several phenylalanine residues (magenta) derived from the opposing dimer molecule (cyan): Phe14, Phe70, Phe73. The electron density is contoured at 0.8σ.

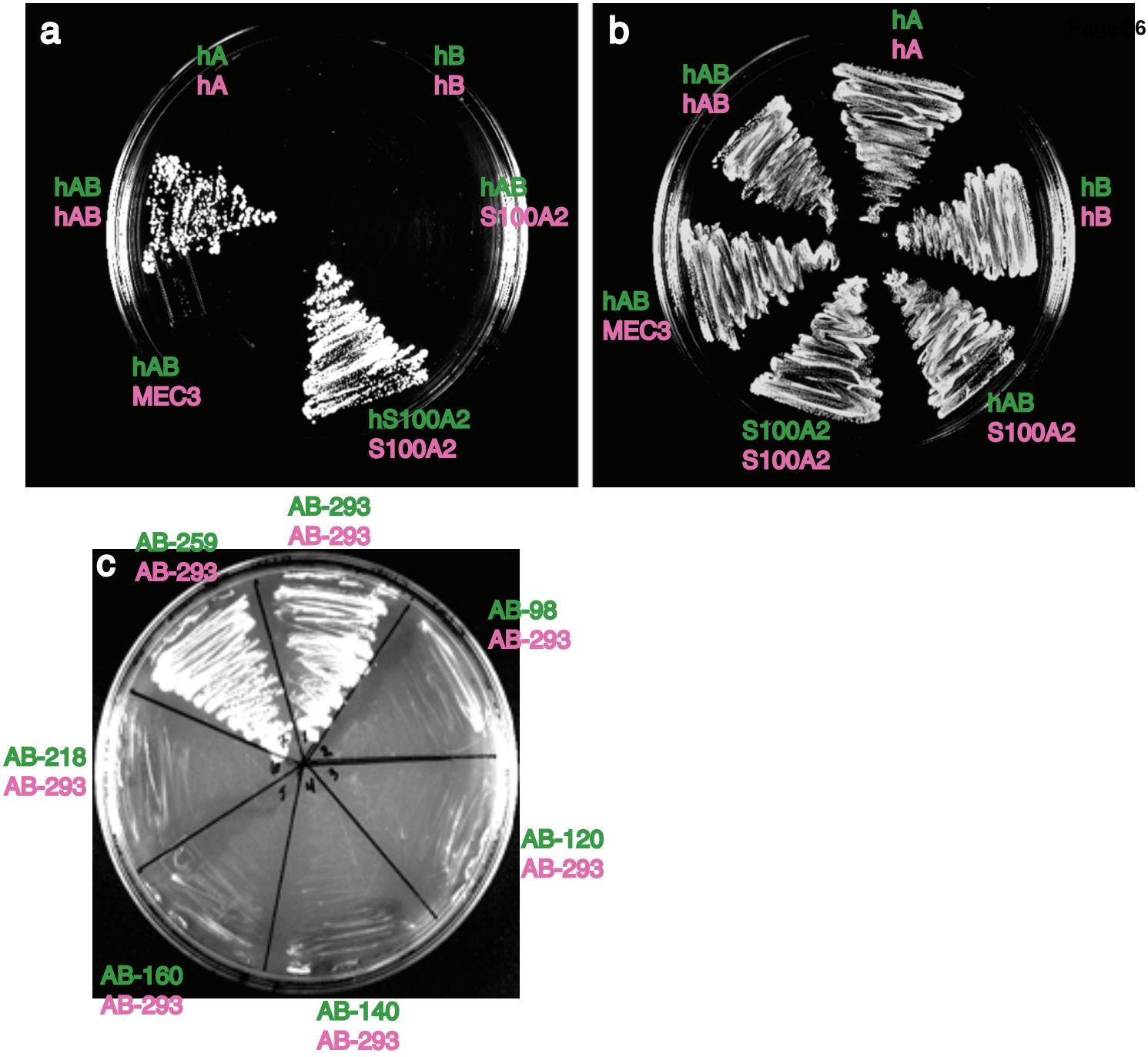

Figure S5. The human profilaggrin N-terminus forms homodimers in yeast.
Human profilaggrin constructs containing either the S100 calcium-binding A domain, B domain or complete N-terminus (A + B domains) prepared in the bait (DNA binding domain) vector (green) or prey (activation domain) (pink) were transformed into yeast, and cells grown on either histidine, leucine and tryptophan (HLT)-deficient media containing 3-amino 1,2,4-triazole (3-AT) (a, c) or leucine and tryptophan(LT)-deficient media as a control (b). Panel (a), bait and prey combinations grown on HLT-deficient containing 5 mM 3-AT. Only the complete terminus (hAB) and the control protein S100A2 formed homodimers in yeast under these selective conditions. Neither human profilaggrin domain A (hA, amino acids 1-91) or B (hB, amino acids 91-293) formed homodimers in yeast. The human AB protein also did not interact with either human S100A2 or yeast MEC3 used as controls. Panel (b), the same bait and prey combinations grown on LT-deficient media, showing robust growth and colony formation. Panel (c), bait and prey human profilaggrin terminus constructs grown on HLT-deficient media with 5 mM 3-AT. Note that the only profilaggrin combinations that interacted in yeast were the AB-293 homodimer containing the complete N-terminus, and the AB-293 in combination with a slightly truncated binding partner, AB-259. The number indicates the number of residues contained in the bait or prey fusion protein. All of the construct combinations grew to confluence on control (LT-deficient) media.

Figure S6. Schematics of constructs used for yeast-two-hybrid analysis of profilaggrin N-terminus homodimerization and N-terminus-annexin II interaction.

Profilaggrin A constructs contain just the S100 domain (residues 1-92), while full-length AB constructs include the complete N-terminus (residues 1-293); additional AB constructs included various truncations made within the B domain, e.g. at residues -98, -120, -140, -160, -218, and -259.

Annexin II (ANXA2) consists of 4 annexin repeats of 70 amino acids (light blue boxes) flanked by N-terminal and C-terminal domains (unshaded boxes). The N-terminal domain of 32 residues includes amino acids 1-14 (shaded black box) that interact with the profilaggrin N-terminus and S100A10.

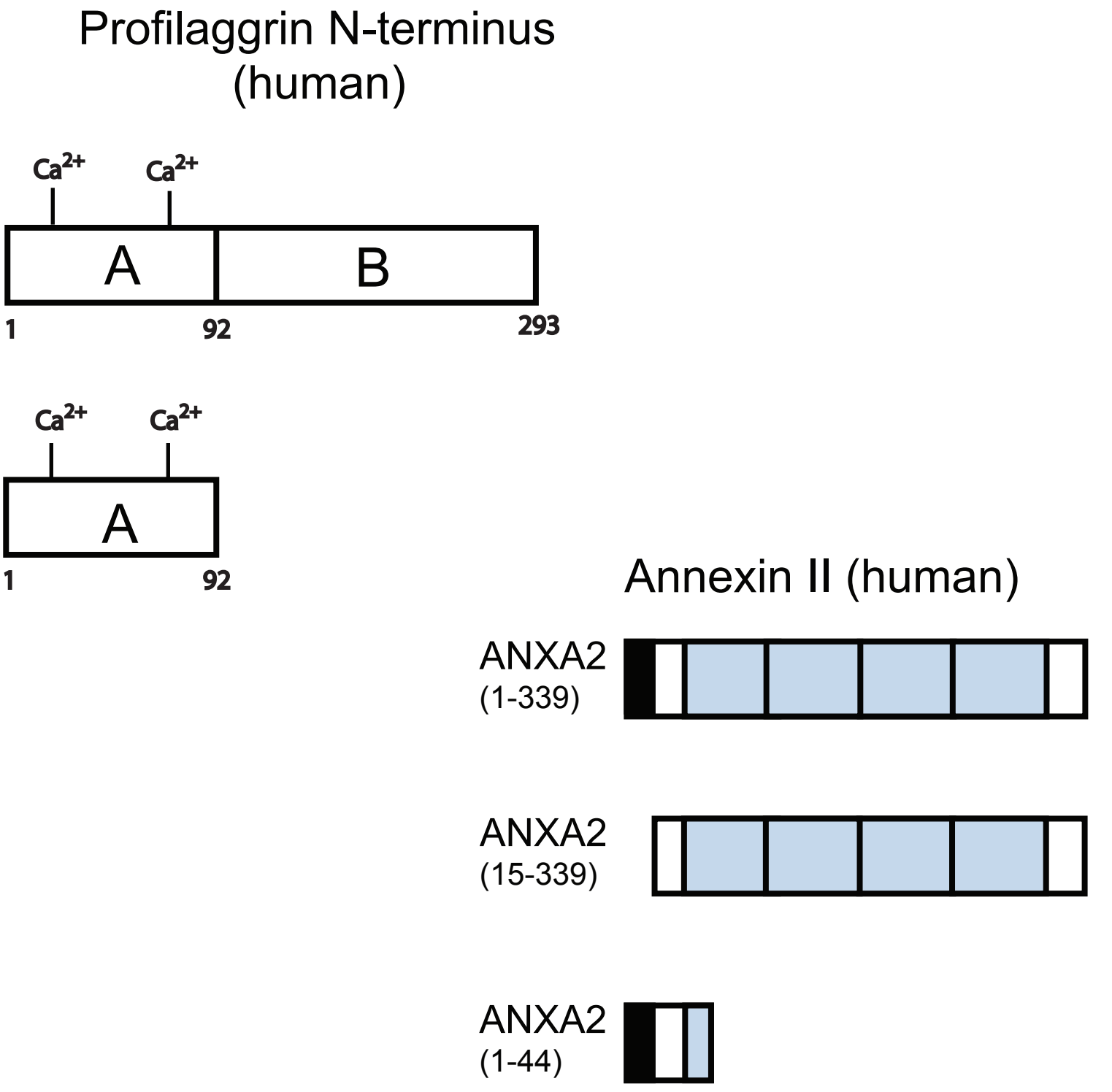

PEG 400 bound in the PF-CABD hydrophobic pocket

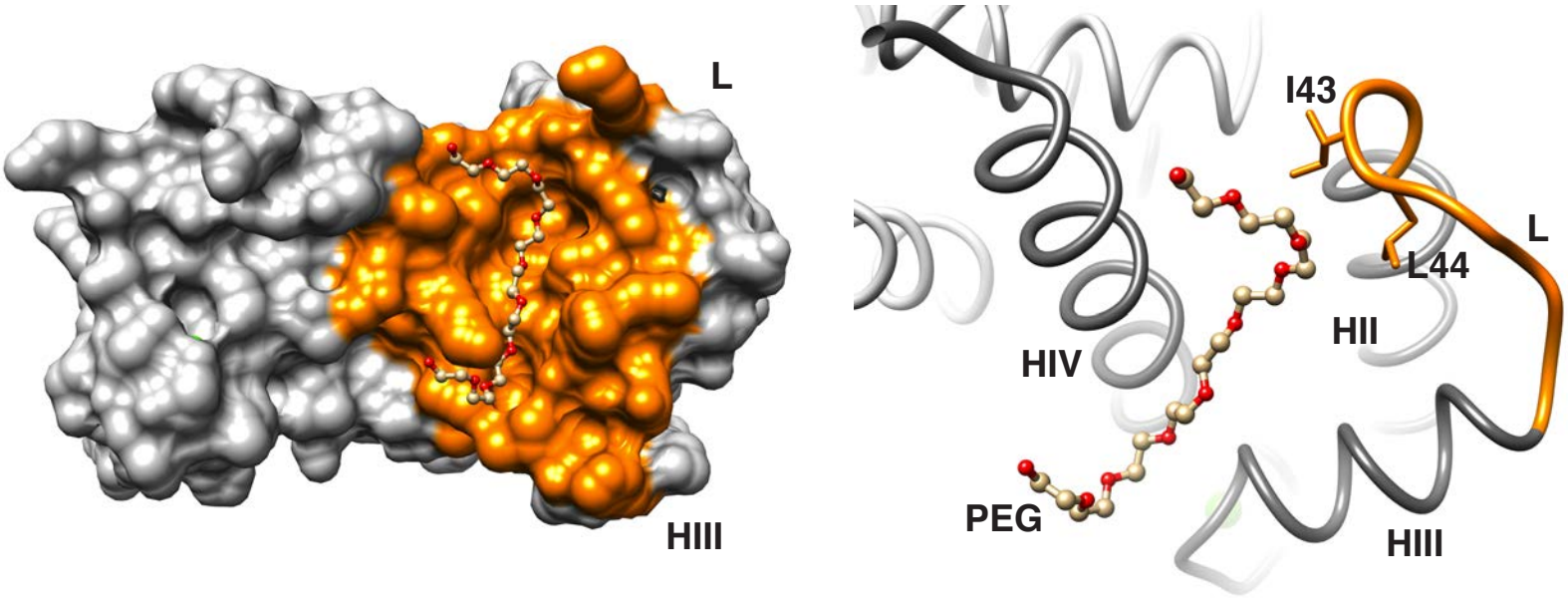

Figure S7 -- PEG 400 binds to the PF-CABD hydrophobic pocket and alters linker conformation.

(Top left) 24 residues (orange) comprise the hydrophobic pocket of one PF-CABD protein, with bound PEG 400 shown as ball and stick model (carbon, white; oxygen, red).

(Top right) Ile43 and Leu44 (side chains orange) contact PEG 400 (carbon, white; oxygen, red), resulting in a folded conformation of inter-EF-hand linker (L). Wire diagram of PF-CABD monomer (gray) with inter-EF-hand linker (orange).

Bound PEG 400 (by-product of cryocrystallography) alludes to the CABD functioning as a target-binding site. Of 24 residues comprising the hydrophobic pocket, 16 interacted with PEG 400 based on analysis of both the “A” and “C” PF-CABD subunits from the crystal AU (Table S2). The “B” and “D” subunits did not contain PEG. Interestingly, only “A” and “C” subunits have linkers between Helix II and Helix III in a “folded” rather than “extended” conformation. Ile43 and Leu44 are positioned centrally in this linker and in the structure contact PEG 400 (above right), suggesting this flexible linker functions to stabilize target interactions. Linker folding likely explains the slightly more “closed” Helix I/II orientation for the “A” and “C” subunits (Table S1).

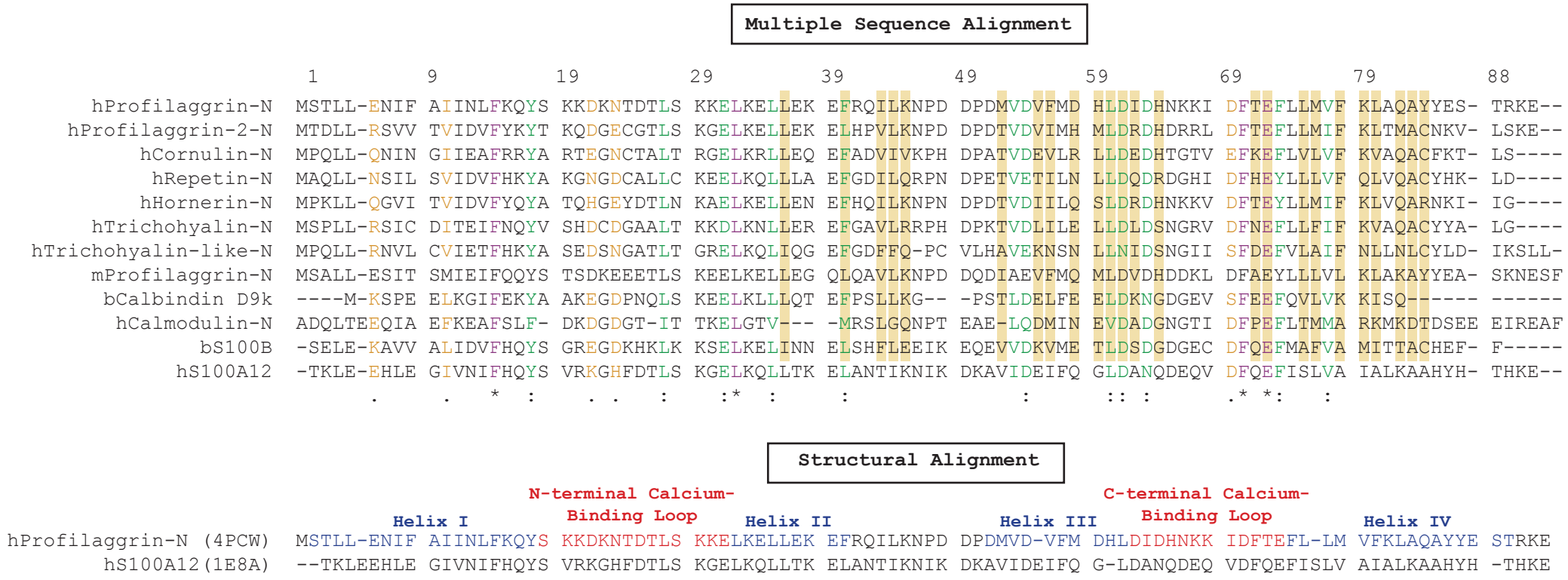

Figure S8.

Clustal Omega multiple sequence alignment (top) of the N-termini of 7 epidermal S100 fused-type proteins as well as calbindin D9k, calmodulin, S100B and S100A12. h = human; m = mouse; b = bovine. Completely conserved residues are colored purple and denoted by (*). Highly conserved residues are colored green and denoted (:). Moderately conserved residues are colored orange and denoted by (.). The numbering across the top represents the amino acid sequence numbering for the crystal structure of profilaggrin N-terminus, not positioning for all aligned sequences. The 24 amino acid residues contributing accessible surface area to profilaggrin's N-terminal hydrophobic pocket have a yellow-shaded background; the shading is extended across the multiple sequence alignment to illustrate differences among the protein sequences.

Swiss-Model structural alignment (bottom) between the crystal structure of the N-terminus of human profilaggrin (PDB Code 4PCW) and human S100A12(PDB Code 1E8A), the latter being the model used for molecular replacement. For the profilagrin structure, helices are labeled and colored blue, whereas calcium-binding loops are labeled and colored red.

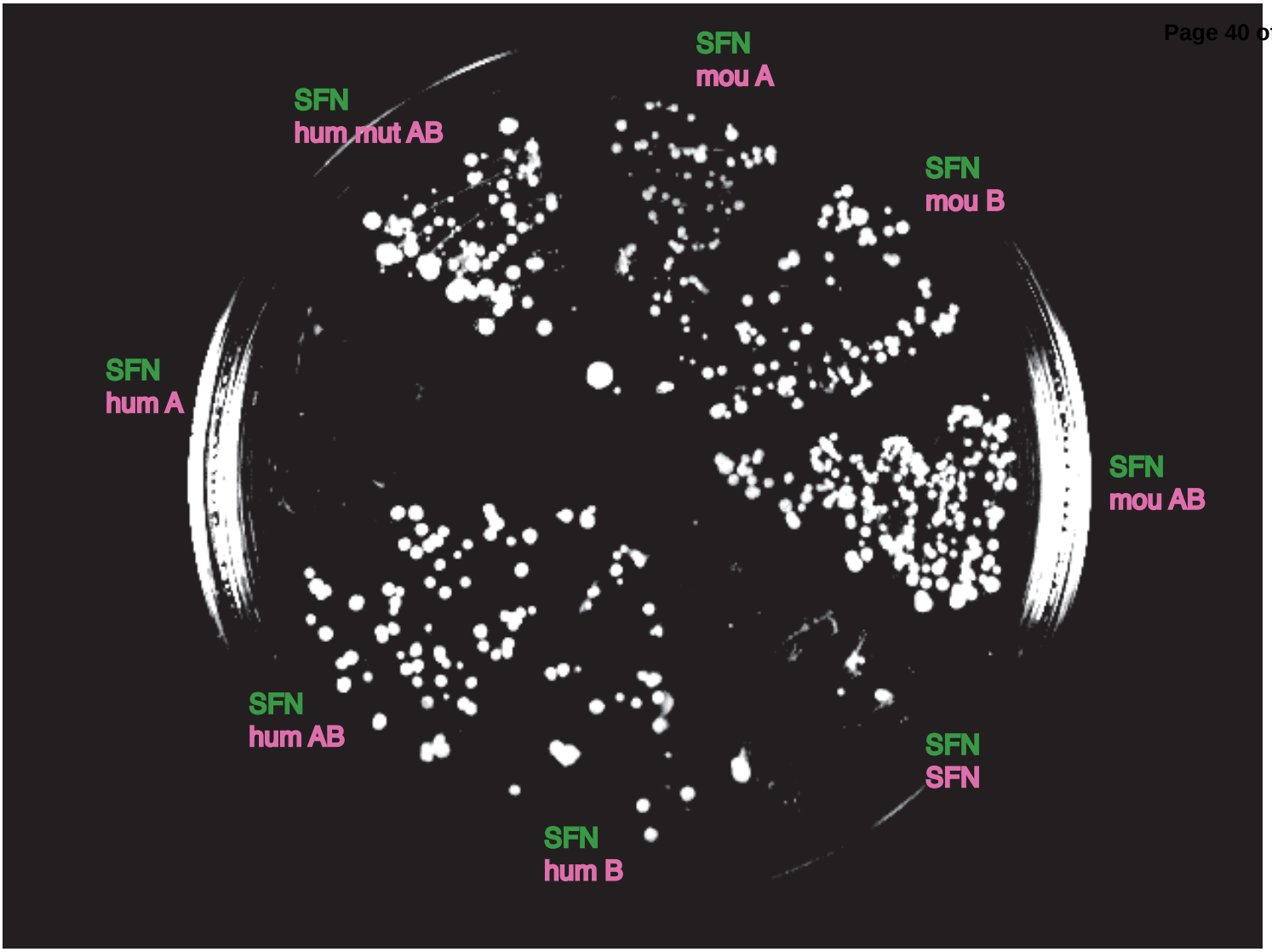

Figure S9, related to Table 2. Stratifin interacts with profilaggrin N-terminus in yeast.
Combinations of bait (green) and prey (pink) fusion proteins were transformed into yeast and grown on HLT-deficient media containing 10 mM 3-AT. Human stratifin (SFN) interacts with full length human profilaggrin N-terminus (hum AB), but not the human A domain (hum A), while SFN interacts with the mouse A and B domains (mou A, B and AB). SFN also gave a similar interaction signal with a mutant human profilaggrin N-terminus protein carrying selected mutations within the calcium-binding domain (hum mut AB). All of the construct combinations grew to confluence on control (LT-deficient) media. Please also see Supplemental Discussion related to this figure.

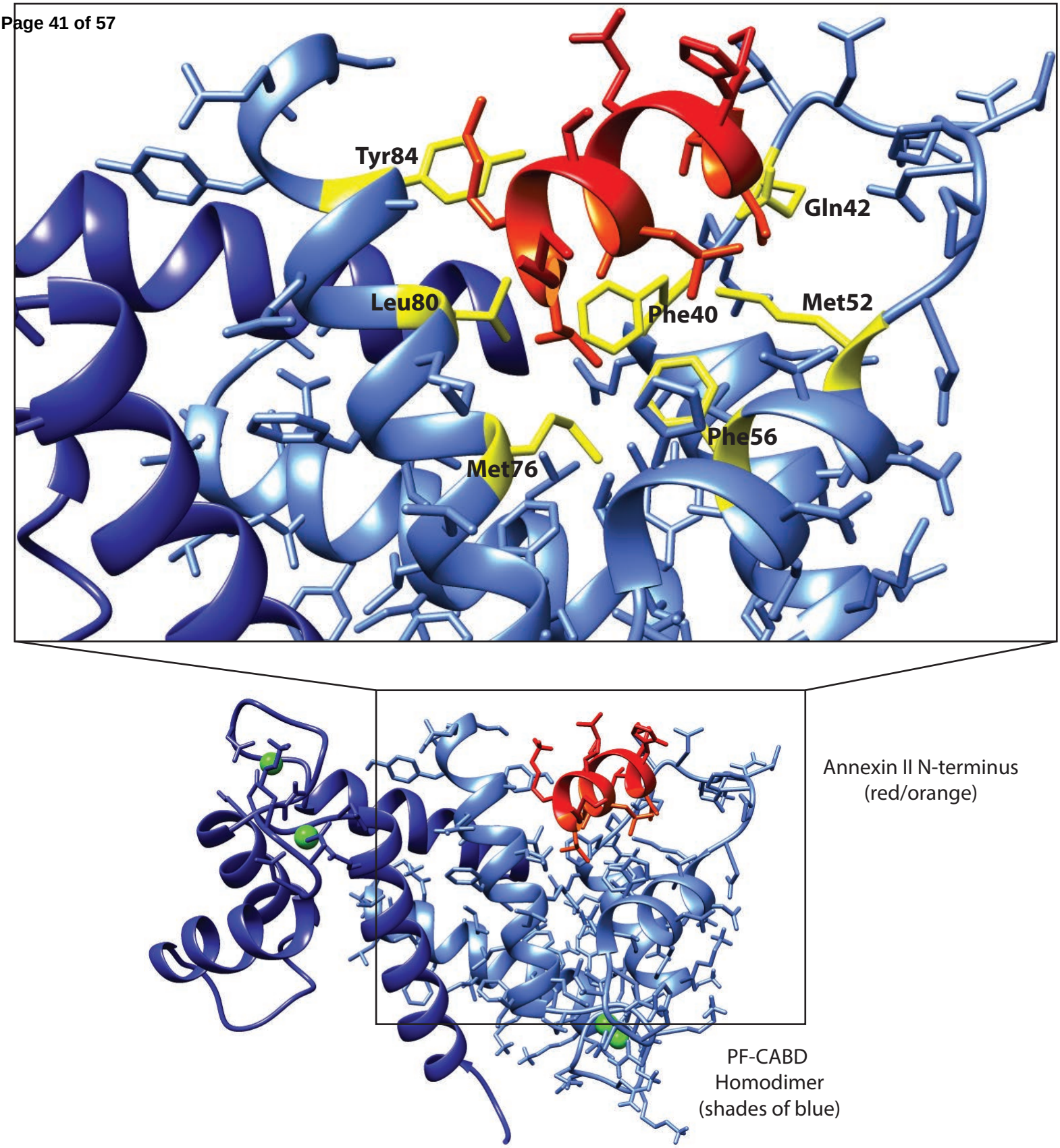

Figure S10. Structural model of PF-CABD binding to annexin II N-terminus from *in silico* molecular docking. The N-terminal 11 residues of *Gallus gallus* annexin II [sequence 1-STVHEILSKLS-11] was molecularly docked onto the PF-CABD dimer structure using the Hex Protein Docking server (http://hexserver.loria.fr/). The structure of the annexin II N-terminus used for docking was dervied from Protein Data Bank Code 1BT6. The sequence differs from human annexin II by a cysteine (human) to serine (chicken) substitution at position 8. Pictured at the bottom is the PF-CABD dimer (light and dark blue) with the annexin II N-terminal helix colored red (the six residues highlighted in orange are the annexin II residues that interact with the PF-CABD binding pocket. In the zoomed in image (top), the seven PF-CABD residues within the hydrophobic pocket that interact with annexin II are highlighted yellow and labeled.

Supplemental Data – Tables

Table S1. Characterization of the interhelical angles and interhelical dimerization contacts of human profilaggrin N-terminal calcium binding domain (PF-CABD).

Interhelical Angles Comparison[a] (°)					
interface					
	I/II	***I/IV***	***II/III***	***II/IV***	***III/IV***
Calbindin D_{9k}	134	126	110	-24	122
Calmodulin-N	88	110	112	-44	85
S100B	136	127	100	-31	103
S100A12 (A)	105	115	89	-24	136
S100A12 (B)	103	119	87	-51	105
PF-CABD (A)	**133**	**135**	**137**	**-28**	**101**
PF-CABD (B)	**123**	**136**	**143**	**-22**	**103**
PF-CABD (C)	**134**	**133**	**139**	**-25**	**102**
PF-CABD (D)	**122**	**136**	**145**	**-23**	**105**

Interhelical Contacts of the Dimerization Interface[b]	
Helical Interface	**Amino Acid Residues**
Helix $I_{A/C}$-Helix $I_{B/D}$	Leu3, Asn6, Ile10, Leu13 ($I_{A/C}$) Leu3, Asn6, Ile10, Leu13 ($I_{B/D}$)
Helix $I_{A/C}$-Helix $IV_{B/D}$	Leu3, Leu4, Ile7, Phe8, Ile11 ($I_{A/C}$) Val77, Leu80, Ala81, Tyr84 ($IV_{B/D}$)
Helix $I_{B/D}$-Helix $IV_{A/C}$	Leu3, Leu4, Ile7, Phe8, Ile11 ($I_{B/D}$) Val77, Leu80, Ala81, Tyr84 ($IV_{A/C}$)
Helix $IV_{A/C}$-Helix $IV_{B/D}$	Phe70, *Thr71*, Leu74, Phe78, *Gln82*, Tyr85 ($IV_{A/C}$) Phe70, *Thr71*, Leu74, Val77, Phe78, Ala81, *Gln82*, Tyr85 ($IV_{B/D}$)

Stabilizing Contacts and Distances (Å) of the N-terminus (Leu3) of Helix I[c]										
	Leu13	Glu39	Phe40	Ile10	Ile7	Val77	Phe73	Met76	Leu35	Leu80
$Leu3_A$	3.74	3.42	3.68	3.93	4.31	4.21	4.47	3.53	5.07	4.63
$Leu3_B$	3.57	4.42	3.22	3.80	3.92	4.14	4.26	5.72	5.38	6.28
$Leu3_C$	3.70	3.44	4.13	4.00	4.26	4.28	4.33	4.59	4.90	4.39
$Leu3_D$	3.57	3.35	3.64	4.23	4.07	4.16	4.14	5.08	4.57	5.50
Average Distance	3.65	3.66	3.67	3.99	4.14	4.20	4.30	4.73	4.98	5.20

[a]Interhelical angles observed in x-ray structures of calcium-bound proteins from the S100 family (PDB Codes 4ICB, 1MHO, 1E8A) and calmodulin (PDB Code 1CLL) are compared to those from all four molecules of PF-CABD (A, B, C, D) in the crystal asymmetric unit (AU). Results demonstrate unique helix I/IV and helix II/III interfaces for PF-CABD.

[b]Amino acid residues playing a key role in the dimerization interface of PF-CABD are listed, with A, B, C, D referring to the four molecules of PF-CABD (two dimers) in the crystal AU. A-B and C-D are the two homodimers, with A analogous to C and B analogous to D. Italics denote that Thr71 and Gln82 hydrogen bond with each other (residues are from opposite dimer molecules) adding to the stability of the two ends of the antiparallel Helix IV plane.

[c]Multiple stabilizing contacts of Leu3 exist at the proximal end of Helix I.

Table S2, related to Figure 2. **Amino Acid Residues Surrounding the Target Binding Pocket and associated Accessible Surface Area.** The asterisks (*) denote residues contacting the bound PEG 400 molecule in either the "A" or "C" subunit from the crystal asymmetric unit. The five residues conserved across the S100 fused-type protein family are denoted (italics, #). A, B, C, D = subunits from the crystal asymmetric unit.

Target Binding Pocket Residues	**Accessible Surface Area** (Å^2)				
HYDROPHOBIC	**A**	**B**	**C**	**D**	**Avg**
Phe40$^{*\#}$	33.96	66.05	30.81	59.30	47.53
Phe56*	26.10	57.60	48.60	38.24	42.64
Phe78	112.62	114.28	114.61	111.23	113.19
Leu36	0.46	8.29	8.70	3.91	5.34
Leu44*	48.75	132.25	51.20	109.85	85.51
Leu60$^{*\#}$	12.45	6.82	15.05	12.56	11.72
Leu75$^{*\#}$	92.51	62.13	87.18	66.06	76.97
Leu80*	42.57	61.45	57.62	59.66	55.33
Ile43*	122.56	150.10	91.40	158.41	130.62
Ile62*	104.98	110.40	102.86	111.98	107.56
Val55	65.18	72.47	73.80	75.99	71.86
Met52*	88.62	91.40	51.48	74.34	76.21
Met76*	17.79	14.42	18.16	12.39	15.69
Ala83$^{*\#}$	62.12	58.27	57.96	67.09	61.36
					901.53 (47.4%)
POLAR					
Tyr84*	123.99	145.31	108.00	144.45	130.44
Thr71	87.92	106.46	90.11	104.27	97.19
Gln82*	143.72	101.82	130.65	107.50	120.92
His59*	118.52	130.17	118.04	125.72	123.11
His64	151.52	143.64	122.16	130.49	136.95
					603.21 (31.8%)
BASIC					
Lys45	18.29	184.03	207.62	167.56	144.38
Lys79*	145.58	109.24	146.73	115.32	129.22
					273.60 (14.4%)
ACIDIC					
Asp58	101.35	112.88	97.59	108.33	105.03
Asp61	8.33	8.32	5.26	3.98	6.47
Glu72$^{*\#}$	6.18	11.10	6.28	13.20	9.19
					120.69 (6.4%)
Total	**1736**	**2059**	**1842**	**1982**	**1899 (100%)**

Table S3, related to Table 2. Identification of three human profilaggrin N-terminus–associated proteins by immunoprecipitation and mass spectrometry[a]

Protein[b]	Amino acid position	Measured Mass	Theoretical Mass	Sequence
Annexin II (12.1%)	104-114	1222.6	1222.6	TPAQYDASELK
	313-323	1421.7	1421.7	SLYYYIQQDTK
	157-175	2080.1	2080.4	DIISDTSGDFRKLMVALAK
Stratifin (10.6%)	130-140	1181.6	1181.6	YLAEVATGDDK
	69-82	1546.7	1546.6	SNEEGSEEKGPEVR
	180-193	1574.0	1572.7	HYEIANSPEEAISL
	101-119	2056.2	2057.3	GLLDSHLIKEAGDAESRVF
Hsp27 (21%)	28-37	1163.6	1163.3	LFDQAFGLPR
	172-188	1906.0	1906.1	LATQSNEITIPVTFESR
	97-112	1783.9	1784.0	VSLDVNHFAPDELTVK

[a] The Genbank accession numbers for these proteins are: NM004039 (ANX2, annexin II/ p36 chain, 338 amino acids); NM006142 (SFN, stratifin/14-3-3sigma, 237 amino acids); and NM001540 (HSPB1 or hsp27, 205 amino acids)

[b] Numbers in parentheses represent % coverage of each protein in the mass spectrometry data

Table S4. **Potential stratifin binding sites at R-X-X-S motifs within the N-terminus of human and mouse profilaggrin.** The amino acid sequence is numbered excluding the N-terminal methionine (leading serine = 1).

Proposed Stratifin Binding Sites of the Profilaggrin N-terminus	
Human	**Mouse**
101-RKHS-104	136-RTRS-139
123-RPSS-126	147-RQES-150
139-RSKS-142	151-RCRS-154
150-RHES-153	178-RHGS-181
258-RSRS-261	241-RADS-244
	264-RQQS-267

Supplemental Materials and Methods

Table S5. Primers used to generate constructs used in yeast two-hybrid studies.

Human profilaggrin N-terminus
Upstream primer
5’ TCT ACT CTC CTG GAA AAC ATC 3’[a]
Downstream primers
5’ TTTTCTGGTAGACTCATAATATGC 3’ (PF-A 91)[b]
5’ TCCTGATATCGGTAAATTCTCTTTTCTGG 3’ (PF-AB 98)
5’ TTCTTTGTTTTCTTCCTGTT 3’ (PF-AB 120)
5’ TCTTCCCTTATTCCCTTTTC 3’ (PF-AB 140)
5’ TTCTTTTTTTTCAGAACTAG 3’ (PF-AB 160)
5’ TTCATAATCATATACTCCTTC 3’ (PF-AB 218)
5’ TCTTTCATATATTTTGTTTTC 3’ (PF-AB 259)
5’ CCTACGCTTTCTTGTCCTGG 3’ (PF-AB 293)
Human B domain construct (amino acids 91-293)
Upstream primer: 5’ AAAGAGAATTTACCGATATCAGG 3’
Downstream primer: 5’ CCTACGCTTTCTTGTCCTGG 3’
Annexin II/p36 constructs
Full length annexin II (339 amino acids)
5’-TCTACTGTTCACGAAATCCTG-3’ (forward)
5’- GTCATCTCCACCACACAGGTA-3’ (reverse)
An N-terminal deletion missing the first 14 amino acids
5’-GATCACTCTACACCCCCAAGT-3’ (forward)
5’- GTCATCTCCACCACACAGGTA-3’ (reverse)
An N-terminal construct containing the first 44 amino acids
5’-TCTACTGTTCACGAAATCCTG-3’ (forward)
5’-GGCTGTTTCAATGTTCAAAGC-3’ (reverse)
Stratifin constructs
Full length human stratifin lacking an initiation codon (247 amino acids)[c]
5’-GAGAGAGCCAGTCTGATCCAG-3’ (forward)
5’-GCTCTGGGGCTCCTGGGGAGC-3’ (reverse)

[a]cDNAs were prepared using the common upstream primer combined with various downstream primers.
[b]Construct names are designated by the C-terminal amino acid present in the expressed protein; for simplicity, engineered restriction sites used for DNA cloning are not shown.
[c]Full length human stratifin lacking an initiation codon (247 amino acids) was cloned into the Y2H vectors pOBD and pOAD.

Supplemental Materials and Methods

Table S6. Profilaggrin Protein Production and Purification Protocol.

1	Human profilaggrin N-terminal calcium binding domain (PF-CABD) was expressed in *Escherichia coli* strain BL21 (DE3) Codon + RIPL (Agilent Technologies) at 37 ^{o}C in Luria Broth Miller (EMD Millipore).
2	Protein expression induced with 1 mM isopropyl-D-thiogalactopyranoside (IPTG) proceeded for 3-4 hours.
3	Cells were harvested by centrifugation at 2500 x g, 10 min., at 4 ^{o}C.
4	The pelleted cells were suspended in 50 mM Tris-HCl buffer (pH 7.8) containing 0.5 M NaCl, 20 mM imidazole, 6 mM $MgCl_2$, 1% Nonidet P-40, and 1x EDTA-free protease inhibitor cocktail (Roche Diagnostics).
5	Cell lysis was achieved by sonication on ice, followed by incubating the solution with ~ 40 units/mL DNase I at 37 ^{o}C for 15 min.
6	The solution was centrifuged at 14000 x g, 15 min, at 4 ^{o}C.
7	The supernatant containing soluble PF-CABD was decanted into a 50 mL centrifuge tube (Corning) containing 5 mL of nickel-NTA agarose (Qiagen) washed with 50 mM Tris-HCl buffer (pH 7.8) containing 0.5 M NaCl and 20 mM imidazole for "batch method" His-tag purification.
8	The solution and nickel resin were incubated for ~ 1 hr at 4 ^{o}C with gentle rocking.
9	The resin was pelleted by centrifugation at 700 x g, 5 min, 4 ^{o}C, and the solution decanted.
10	The resin was suspended in 30 mL of 50 mM Tris-HCl buffer (pH 7.8) containing 0.5 M NaCl and 20 mM imidazole, allowed to "wash" for 10-15 min. at 4 ^{o}C with gentle rocking, then the resin was pelleted again at 700 x g, 5 min., at 4 ^{o}C with decanting of the supernatant.
11	The wash cycle was repeated a second time, after which the pelleted nickel resin containing bound His-tagged PF-CABD was incubated overnight with 15.2 μg (34 units) bovine alpha-thrombin (Haematologic Technologies, Inc.) at 20 ^{o}C to remove the His-tag.
12	The following morning the resin was suspended to 5 mL with 50 mM Tris-HCl buffer (pH 7.8) containing 0.5 M NaCl and 20 mM imidazole, and syringe-filtered through a 0.45 μm filter (EMD Millipore) to remove the nickel resin bound to His-tag.
13	The clarified solution containing the untagged PF-CABD was applied to a Superdex 75 (26/60) gel filtration column for further purification in either 50 mM Tris-HCl buffer (pH 7.8) containing 0.5 M NaCl and 5 mM $CaCl_2$ (size exclusion chromatography experiments) or 50 mM Tris-HCl buffer (pH 7.8) containing 0.5 M NaCl and 1 mM EDTA (size exclusion chromatography, light scattering, crystallization experiments).
14	Collected fractions were analyzed by sodium dodecyl sulfate polyacrylamide gel electrophoresis (SDS-PAGE), and selected pooled fractions were concentrated in a 3000 Da molecular weight cutoff centrifugal filter unit (EMD Millipore) prior to crystallization.

Supplemental Materials and Methods

Profilaggrin constructs

For Y2H, human profilaggrin N-terminal constructs containing the A (S100) domain, B domain or A domain plus varying amounts of the B domain were prepared using PCR and DNA cloning into the pOBD and pOAD vectors (Yeast Resource Center, University of Washington) (Hudson *et al.*, 1997) (Table S5). For crystallization, PF-CABD (A domain, human profilaggrin residues 1-92 inclusive of N-terminal methionine) was purchased from GenScript (Piscataway, NJ) (transformed into plasmid pGS-21a) containing N-terminal 6x-histidine tag with thrombin cleavage site. PF-CABD was sequence verified by DNA sequencing at the Keck Biotechnology Resource Laboratory (Yale University, New Haven, CT). Mouse profilaggrin N-terminal constructs encoding 99 amino acids (A domain) and 283 amino acids (A and B domains) were prepared as described (Yoneda *et al.*, 2012).

Annexin II (p36) and stratifin constructs

Full length human cDNA for annexin II (p36) was generated by RT-PCR from foreskin cDNA with customized primers using standard procedures (Presland *et al.*, 2000) and the DNA products cloned into TOPO-TA vector (Life Technologies, Grand Island, NY) (Table S5). A human stratifin (14-3-3sigma) cDNA clone was obtained from Dr. Michael Yaffe (MIT, Boston) (Table S5). All PCR products were cloned in-frame into the Y2H vectors pOBD and pOAD; miniprep plasmid DNA was sequence verified prior to

transformation into yeast. Two additional control cDNAs for Y2H experiments, human S100A2 and yeast MEC3, were gifts of Drs. J.T. Elder and S. Fields, respectively.

Yeast two-hybrid assays and expression analysis.

Plasmids were transformed into yeast strain PJ694A (Yeast Resource Center) using a commercial yeast transformation kit (Zymo Research, Orange, CA) as described previously (Yoneda *et al.*, 2012). Double-transformed yeast stocks containing pOBD and pOAD plasmids were maintained on tryptophan and leucine-deficient yeast (LT) plates. For yeast two-hybrid assays, cells were plated on histidine-deficient plates (also lacking tryptophan and leucine, designated HLT plates) containing between 2.5 and 20 mM 3-amino-1,2,4-triazole (3-AT) (Sigma-Aldrich, St. Louis, MO) and grown at 30 ºC.

For protein expression analysis, yeast cells containing either one or two plasmids were grown overnight in selective yeast media (lacking either leucine, or leucine and tryptophan) and yeast protein lysates were prepared using glass beads, as recommended by Clontech (Palo Alto, CA). Alternatively, yeast cells were pelleted in a microfuge and directed lysed into SDS loading buffer, prior to loading on SDS/polyacrylamide gels (Warner *et al.*, 2000). SDS/PAGE and Western blotting of yeast lysates (~25 µg/lane) were performed as described previously, using either human profilaggrin N-terminal antibodies to assess the expression of bait and prey hybrid proteins. Immunoblots were developed by ECL using SuperSignal West Pico substrate (ThermoFisher Scientific, Rockford, IL). A human foreskin Urea/Tris extract was used as a positive control for immunoblots.

Immunoprecipitation and mass spectrometry.

Human neonatal foreskin epidermis was separated from underlying dermis and homogenized in a modified RIPA buffer containing 1% Nonidet P-40 (Pearton *et al.*, 2001). Human profilaggrin B1 antibody (Presland *et al.*, 1997) or an irrelevant polyclonal IgG control antiserum (10 μg) was conjugated to 100 ml of protein A-conjugated paramagnetic Dynabeads® (Dynal Biotech, Carlsbad, CA) in 50 mM Tris-HCl pH 8.1 by incubation for 20 min at room temperature. Beads were washed three times in the same Tris buffer and incubated with 1 ml of foreskin lysate (~ 1 mg total protein) overnight at 4 °C with gentle shaking. After extensive washing with PBS the immunoprecipitated antigens were eluted with 50 mM glycine pH 2.8 and the eluate neutralized with 0.5 M Tris. Immunoprecipitation of the profilaggrin N-terminal peptide was confirmed by SDS/PAGE of a small portion of the total eluted material and western blotting with profilaggrin A or B1 antibody as described (Presland *et al.*, 1997).

The remainder of the immunoprecipitate was separated on a 7.5-12.5% SDS/polyacrylamide gel and stained with Coomassie Brilliant Blue (CBB) solution. Protein bands were excised from the gel, destained, and in-gel digested with mass spectrometry grade trypsin (Sigma) (Shevchenko *et al.*, 1996). Peptides were eluted from the gel, dried in a Speedivac and the mixtures analyzed using a triple quadrupole mass spectrometer (TSQ 7000, Finnegan Mat, San Jose, CA) with an in-house fabricated electrospray source and a HP 1100 solvent delivery system (Hewlett Packard, Palo Alto,

CA). Peptide identification was obtained from collision-induced dissociation mass spectra using SEQUEST (The Scripps Research Institute, La Jolla, CA).

Immunoprecipitation experiments to confirm protein-protein interactions in tissue lysates were performed as described previously (Pearton *et al.*, 2002), except that in some cases 5 mM $CaCl_2$ or 5 mM EDTA was added to the incubation containing primary antibody and tissue lysate. Immunoprecipitated proteins were eluted from protein A-conjugated paramagnetic beads as described above, and the entire eluate was run on SDS/polyacrylamide gels, transferred to PVDF membrane and immunoblotted with antibody.

Immunofluorescence microscopy.

For immunolocalization studies, human adult skin was cryosectioned at a thickness of 6 μm and fixed in 4% paraformaldehyde. Sections were immunolabeled with a rabbit antibody to human profilaggrin (B1)(1:1000) and a goat antibody to human stratifin (1:16) as described (Presland *et al.*, 1997; Underwood *et al.*, 2009). After labeling with primary antibodies, sections were subsequently labeled with a biotinylated donkey anti-goat IgG and streptavidin-Texas Red to visualize stratifin, and a donkey anti-rabbit IgG conjugated with fluorescein isothiocyanate (Jackson ImmunoResearch, West Grove, PA) to visualize profilaggrin. Tissue sections were counterstained with 4′,6-diamidino-2-phenylindole (DAPI) to identify nuclei. Tissue sections were visualized using a Nikon Microphot-SA upright microscope equipped with both transmitted and epi-fluorescence illumination (Nikon Instruments; Melville, NY). Images were acquired using a

Photometrics digital camera (Roper Scientific/Photometrics, Tucson, AZ). To identify cells where protein co-localization occurred, image multiplication was performed using the Image Processing Tool Kit within Photoshop. Eight-bit digital files captured with individual green and red filters were merged, and the resulting multiplied pixel intensity, representing immunolocalization, was saved as a Photoshop file.

Statement on Use of Human Materials.

Normal human neonatal and adult skin, utilized for immunofluorescence microscopy and immunoprecipitation studies, were obtained through the Division of Dermatology with approval from the University of Washington Institutional Review Board.

Hudson JR, Dawson EP, Rushing KL*, et al.* (1997) The complete set of predicted genes from Saccharomyces cerevisiae in a readily usable form. *Genome Res* 7:1169-73.

Pearton DJ, Dale BA, Presland RB (2002) Functional analysis of the profilaggrin N-terminal peptide: identification of domains that regulate nuclear and cytoplasmic distribution. *J Invest Dermatol* 119:661-9.

Pearton DJ, Nirunsuksiri W, Rehemtulla A*, et al.* (2001) Proprotein convertase expression and localization in epidermis: evidence for multiple roles and substrates. *Exp Dermatol* 10:193-203.

Presland RB, Boggess D, Lewis SP*, et al.* (2000) Loss of normal profilaggrin and filaggrin in flaky tail (ft/ft) mice: an animal model for the filaggrin-deficient skin disease ichthyosis vulgaris. *J Invest Dermatol* 115:1072-81.

Presland RB, Kimball JR, Kautsky MB*, et al.* (1997) Evidence for specific proteolytic cleavage of the N-terminal domain of human profilaggrin during epidermal differentiation. *J Invest Dermatol* 108:170-8.

Shevchenko A, Wilm M, Vorm O*, et al.* (1996) Mass spectrometric sequencing of proteins silver-stained polyacrylamide gels. *Anal Chem* 68:850-8.

Underwood RA, Carter WG, Usui ML*, et al.* (2009) Ultrastructural localization of integrin subunits beta4 and alpha3 within the migrating epithelial tongue of in vivo human wounds. *J Histochem Cytochem* 57:123-42.

Warner AJ, Lopez-Dee J, Knight EL*, et al.* (2000) The Shc-related adaptor protein, Sck, forms a complex with the vascular-endothelial-growth-factor receptor KDR in transfected cells. *Biochem J* 347:501-9.

Yoneda K, Nakagawa T, Lawrence OT*, et al.* (2012) Interaction of the profilaggrin N-terminal domain with loricrin in human cultured keratinocytes and epidermis. *J Invest Dermatol* 132:1206-14.

Supplemental Discussion to Figure 3 and Supplemental Figure S9.

Annexin II binds S100A10 (Zobiack *et al.*, 2001), protecting it from ubiquitin-mediated degradation (He *et al.*, 2008) and modulating proteolytic activity of plasmin (Madureira *et al.*, 2012). The angiogenic and tumor-associated protein S100A4 also binds annexin II, probably via the same N-terminal region (Semov *et al.*, 2005). Elevated levels of pro-inflammatory plasmin and annexin II were found in psoriatic skin (Li *et al.*, 2011), and 30-fold elevated plasmin levels were seen in acute atopic dermatitis skin (Voegeli *et al.*, 2009). Additional functions of annexin II include regulation of cellular growth, signal transduction, anionic phospholipid binding, and linkage of membrane-associated proteins to the actin cytoskeleton (Bharadwaj *et al.*, 2013). While we were unable to find solid evidence that annexin II and profilaggrin co-localize in the granular layer by double-label immunofluorescence, it is still possible that annexin II and the profilaggrin N-terminus interact transiently during terminal differentiation, for example during cornified envelope assembly where other S100 proteins and annexins play a role (Robinson *et al.*, 1997).

Stratifin has multiple functions regulating the epidermal cell cycle, epithelial keratinization, and keratinocyte differentiation. It is highly expressed in differentiated keratinocytes, and recent studies in transgenic mice suggest it decreases keratinocyte proliferation by functioning as an “epidermal proliferation differentiation switch” (Voegeli *et al.*, 2009). These findings are consistent with

studies on the N-terminus of profilaggrin that show it inhibits keratinocyte growth and development, acting as a negative feedback mechanism on epidermal homeostasis (Aho *et al.*, 2012). In many cases 14-3-3 proteins regulate the function of their binding partners by restricting them to a particular subcellular compartment and/or by masking certain functional domains (van Hemert *et al.*, 2001). Homozygous repeated epilation (Er/Er) mice, which contain a mutation in the stratifin gene, exhibit abortive differentiation, which demonstrates the importance of this protein as a positive regulator of normal terminal differentiation, particularly the expression of stratum granulosum markers including filaggrin, as well as barrier formation (Li *et al.*, 2005). For profilaggrin N-terminus, it is possible that stratifin, which is predominantly cytoplasmic, acts to restrict the nuclear translocation of PF-NT after it is processed from profilaggrin, as PF-AB is generally only seen in vivo in the nucleus of dying cells that are transitioning to corneocytes (Ishida-Yamamoto *et al.*, 1998). Such a role for stratifin is consistent with the co-localization of it and the profilaggrin N-terminus in the cytoplasm of epidermal granular cells (see Figure 4).

Aho S, Harding CR, Lee JM*, et al.* (2012) Regulatory role for the profilaggrin N-terminal domain in epidermal homeostasis. *J Invest Dermatol* 132:2376-85.

Bharadwaj A, Bydoun M, Holloway R*, et al.* (2013) Annexin A2 heterotetramer: structure and function. *Int J Mol Sci* 14:6259-305.

He KL, Deora AB, Xiong H*, et al.* (2008) Endothelial cell annexin A2 regulates polyubiquitination and degradation of its binding partner S100A10/p11. *J Biol Chem* 283:19192-200.

Ishida-Yamamoto A, Takahashi H, Presland RB*, et al.* (1998) Translocation of profilaggrin N-terminal domain into keratinocyte nuclei with fragmented DNA in normal human skin and loricrin keratoderma. *Lab Invest* 78:1245-53.

Li Q, Ke F, Zhang W*, et al.* (2011) Plasmin plays an essential role in amplification of psoriasiform skin inflammation in mice. *PLoS One* 6:e16483.

Li Q, Lu Q, Estepa G*, et al.* (2005) Identification of 14-3-3sigma mutation causing cutaneous abnormality in repeated-epilation mutant mouse. *Proc Natl Acad Sci U S A* 102:15977-82.

Madureira PA, O'Connell PA, Surette AP*, et al.* (2012) The biochemistry and regulation of S100A10: a multifunctional plasminogen receptor involved in oncogenesis. *J Biomed Biotechnol* 2012:353687.

Robinson NA, Lapic S, Welter JF*, et al.* (1997) S100A11, S100A10, annexin I, desmosomal proteins, small proline-rich proteins, plasminogen activator inhibitor-2, and involucrin are components of the cornified envelope of cultured human epidermal keratinocytes. *J Biol Chem* 272:12035-46.

Semov A, Moreno MJ, Onichtchenko A*, et al.* (2005) Metastasis-associated protein S100A4 induces angiogenesis through interaction with Annexin II and accelerated plasmin formation. *J Biol Chem* 280:20833-41.

van Hemert MJ, Steensma HY, van Heusden GP (2001) 14-3-3 proteins: key regulators of cell division, signalling and apoptosis. *Bioessays* 23:936-46.

Voegeli R, Rawlings AV, Breternitz M*, et al.* (2009) Increased stratum corneum serine protease activity in acute eczematous atopic skin. *Br J Dermatol* 161:70-7.

Zobiack N, Gerke V, Rescher U (2001) Complex formation and submembranous localization of annexin 2 and S100A10 in live HepG2 cells. *FEBS Lett* 500:137-40.

AUTHOR CONTRIBUTIONS

C.G.B. designed and conducted the crystallography study, including purification and crystallization of the protein; collection, processing, and refinement of the crystallographic data; structural analysis, gel filtration and light scattering studies; wrote the manuscript. Yeast two-hybrid, immunoprecipitation, mass spectrometry, and cell biology studies were performed by O.T.L., D.J.P., and R.B.P; L.M.M. and T.A.S. aided in experimental design, analyzed the data, and provided guidance. All authors contributed to the writing of the manuscript, and approved the final version.